Progress In Electromagnetics Research M, Vol. 44, 47–58, 2015

Single-Antenna Time-Reversal Imaging Based on Independent Component Analysis

Payman Rasekh, Mojtaba Razavian, Amir Torki, Hossein K. Rad, and Reza Safian*

Abstract—Time reversal techniques are based on the time reversal invariance of the wave equation. They use time-reversed fields recollected by an array antenna to perform imaging and focusing on the source of received signals. Two widely used time reversal techniques are DORT and time reversal MUSIC which are based on eigenvalue decomposition of the time reversal operator. We introduce a new time reversal technique based on independent component analysis (ICA). Time reversal ICA (TR-ICA) exploits the independence of scattered signals of the well-resolved targets to perform imaging. It breaks the mixed backscattered received signals to independent components by maximizing the non-Gaussianity of basic signals. The main advantage of this method is that imaging and focusing are achieved using only one transmitting antenna which simplifies the physical implementation drastically. We have simulated the performance of the introduced method in different scenarios such as selective focusing in the presence of scatterers with different materials, sizes and distances. In addition, the effect of noise on TR-ICA and through-the-wall imaging (TWI) are studied. Some of the results are compared to the DORT method. Finally, the validity of this algorithm is verified by performing physical measurements.

1. INTRODUCTION

In acoustic domain time-reversal (TR) techniques have shown to provide promising results for the detection and localization of scatterers in multiple-scattering environments [1, 2]. These techniques are based on time reversal invariance of the wave equation in lossless and stationary medium. Their implementation involves retransmission of scattered signals acquired by a set of receivers in a time-reversed fashion. Retransmitted time-reversed signals propagate backwards through the same medium and experience similar multiple scattering, reflections and refractions which the signals have gone through during the forward propagation, resulting in energy focusing around the initial source locations. With the success of initial TR experiments in acoustics, there has been strong interest in the application of TR methods using radio frequency electromagnetic waves [3–5].

There are different methods used to implement time reversal imaging. The most common methods are time domain DORT [6], time reversal MUSIC [7], single frequency DORT [8] and single frequency MUSIC [9]. These methods differ mainly in the construction of the multi-static data matrix (MDM) and the usage of eigenvalues and eigenvectors in order to focus on the desired scatterer. One of the drawbacks of these two methods is that the number of transmitting and receiving antennas must be more than the number of scatterers in the medium. Since usually we do not have any information about the number of scatterers, we have to select the number of transmitting and receiving antennas as large as possible, which leads to high computation complexity.

Hence, due to the need for large number of transmitter and receivers, physical implementation of the current time reversal techniques is expensive and in many cases not practically feasible. We have introduced a new method for microwave imaging using TR technique in which independent of the number

Received 17 July 2015, Accepted 28 September 2015, Scheduled 8 October 2015
* Corresponding author: Reza Safian (rsafian@cc.iut.ac.ir).
The authors are with the Electrical and Computer Engineering Department, Isfahan University of Technology, Isfahan 84156, Iran.

of scatterers, only one transmitting antenna and an array of receiving antennas are needed for detection and focusing on the desired scatterer(s). This simplifies the physical implementation of the microwave imaging method compared to other techniques. We have used independent component analysis (ICA) to manipulate the time reversal data (TR-ICA) [10–13]. In this method, the construction of multi-static data matrix and the derivation of scatterers information are different from both DORT and MUSIC methods and are done in time-domain. Basically, independent component analysis (ICA) is an algorithm which breaks mixed signals to basic independent signals [14]. There are different implementations of independent component analysis to calculate the independent signals. Some of these methods are Gradient algorithm, infomax [15], Jade [16] and FastICA [17]. The FastICA algorithm has the cubic coherent property and is faster and more accurate than the others. We have chosen the FastICA algorithm to apply this method in a continuously random medium.

In this paper, propagation and scattering of the electromagnetic waves are simulated using two-dimensional finite difference method. The scatterers are placed in an inhomogeneous medium with spatially fluctuating random permittivity and prescribed correlation function [6, 18]. Target identification in the case multiple clutter objects are present is investigated. The effect of noise and direction of the target with respect to the transmitting antenna are simulated. One of the challenges of any microwave imaging technique is the through-the-wall scenario in which the targets and the transmitting and receiving antennas are on opposite sides of a wall. We have also shown the results of a through-the-wall imaging example. To prove the effectiveness of the method, we have performed physical experiments in which selective focusing is done using TR-ICA method.

2. INDEPENDENT COMPONENT ANALYSIS (ICA)

A fundamental problem in signal processing is finding a suitable representation of multivariate data, i.e., random vectors. Well-known linear transformation methods are principal component analysis, factor analysis, and projection pursuit. In independent component analysis (ICA), the goal is to find a linear representation of non-Gaussian data so that the components are statistically independent or, as independent as possible. Such a representation seems to capture the essential structure of the data in many applications including feature extraction and signal separation [12–15].

Assuming that we have N_s signal sources $(s_1(t), s_2(t), \ldots, s_{N_s}(t))$ and N_r receivers, therefore, we will have N_r observation vectors in time $(k_1(t), k_2(t), \ldots, k_{N_r}(t))$. Assuming that received signals are a linear mixture of independent source signals, therefore,

$$\begin{pmatrix} k_1(t) \\ k_2(t) \\ \vdots \\ k_{N_r}(t) \end{pmatrix} = \mathbf{A} \begin{pmatrix} s_1(t) \\ s_2(t) \\ \vdots \\ s_{N_s}(t) \end{pmatrix} \tag{1}$$

The observation matrix $\mathbf{K}$ is a $N_r \times N_t$ matrix, and source matrix $\mathbf{S}$ is $N_s \times N_t$. Matrix $\mathbf{A}$ is a $N_r \times N_s$ matrix which is known as the mixing matrix. It relates the received and transmitted signals. N_t is the number of time samples. Having the observation matrix $\mathbf{K}$, independent component analysis estimates both matrix $\mathbf{A}$ and the $\mathbf{S}$. In general, the number of independent sources (N_s) and the number of observation signals (N_r) are not necessarily equal [13, 14]. However, for the ICA algorithm to work properly, N_r must be equal to or greater than N_s.

Alternatively, we could define ICA as a linear transformation given by a matrix $\mathbf{B}$ as in

$$\begin{pmatrix} y_1(t) \\ y_2(t) \\ \vdots \\ y_{N_s}(t) \end{pmatrix} = \mathbf{B} \begin{pmatrix} k_1(t) \\ k_2(t) \\ \vdots \\ k_{N_r}(t) \end{pmatrix} \tag{2}$$

So that the random variables y_i, $i = 1, \ldots, N_s$ are as independent. Matrices $\mathbf{A}$ and $\mathbf{B}$ are related by an inverse relation. We can show this linear combination as

$$\mathbf{Y} = \mathbf{BK} \tag{3}$$

$$y_i = \sum_j b_{ij} k_j \tag{4}$$

where $\mathbf{B}$ has to be determined. However, we can denote $\mathbf{BA}$ by $\mathbf{Q}$. Therefore, we have

$$\mathbf{Y} = \mathbf{B}(\mathbf{AS}) = \mathbf{QS} \tag{5}$$

$$y_i = \sum_j q_{ij} s_j \tag{6}$$

The idea is that according to the central limit theorem sums of non-Gaussian random variables are closer to Gaussian that the original ones. Therefore, if we take a linear combination $y_i = \sum_j b_{ij} k_j$ of the observed mixture variables (which, because of the linear mixing model, is a linear combination of the independent components as well), this will be maximally non-Gaussian if it equals one of the independent components. It means that by finding local maxima of non-Gaussianity of y, the independent components, i.e., s_is, are achieved.

Non-Gaussianity is zero for Gaussian random variables and nonzero for other random distributions. We have used negentropy as a measurement tool for non-Gaussianity. Negentropy is based on the information of theoretic quantity of entropy. A fundamental result of information theory is that a Gaussian random variable has the largest entropy among all random variables. Negentropy is defined as

$$J(y) = H(y_{\text{gauss}})H(y) \tag{7}$$

where y_{gauss} is a Gaussian random variable with covariance equal to random variable y, and H is the entropy. Gaussian variables have the largest entropy, thus, negentropy is always greater than zero and equal to zero for Gaussian variables. It is not easy to measure negentropy accurately. Therefore, we use an approximation of negentropy which is defined as

$$J(y) \approx t_1 E\left\{G^1(y)\right\}^2 + t_2 E\left\{G^2(y)\right\}^2 - E\left\{G^2(\nu)\right\}^2 \tag{8}$$

where ν is a Gaussian random variable with unit variance and zero mean, y also a random variable with unit variance and zero mean, and t_1 and t_2 are positive constants. $G^1(y)$ and $G^2(y)$ are nonlinear functions usually defined as ($1 \le a_1 \le 2$ is constant)

$$G^1(y) = \frac{1}{a_1}\log\left(\cosh(a_1 y)\right), \quad G^2(y) = -\exp\left(-y^2/2\right) \tag{9}$$

We have to perform two preprocessing steps on observation data $\mathbf{K}$, i.e., centering and whitening [12]. The algorithm we use here for computation of the ICA model is the FastICA algorithm. It is based on a fixed-point iteration scheme for finding the maximum of the non-Gaussianity. The following algorithm shows the computation process.

1) Centering the observation matrix $\mathbf{K}$. 2) Whitening the matrix to compute Q. 3) Choosing the number of independent components, m, and setting $p = 1$. 4) Choosing an initial value for $\mathbf{b}_p$ with unit norm. 5) Letting $\mathbf{b}_p \leftarrow E\{\mathbf{q}g(\mathbf{b}_p^T\mathbf{q})\} - E\{g'(\mathbf{b}_p^T\mathbf{q})\}\mathbf{b}$, where g is the derivation of the functions $G(y)$ defined above and g' the derivation of g as in the following equations

$$g_1(y) = \tanh(a_1 y), \quad g_2(y) = y\exp(y^2/2). \tag{10}$$

6) Doing the orthogonalization $\mathbf{b}_p \leftarrow \mathbf{b}_p \sum_{j=1}^{p-1}((\mathbf{b}_p^T\mathbf{b}_j)\mathbf{b}_j)$. 7) Letting $\mathbf{b}_p \leftarrow \mathbf{b}_p/||\mathbf{b}_p||$. 8) If $\mathbf{b}_p$ is not converged, go back to 5. 9) Letting $p \leftarrow p+1$, and if $p \le m$, go back to 4.

We should notice that convergence in above algorithm means that old and new values for vectors $\mathbf{b}_i$ ($i = 1, \ldots, N_s$) point in the same direction. The convergence of above iterative algorithm is cubic. The performance of the FastICA algorithm can be optimized by choosing a suitable nonlinear function G in the preceding algorithm. The algorithm above computes the orthogonal vectors $\mathbf{b}_i$ one by one by using the Gram-Schmidth in step 6. Performing ICA on $\mathbf{K}$ provides us with N_s independent vectors ($\mathbf{a}_j$, $j = 1 : N_s$), and each of them is $N_r \times 1$. Each vector denotes a column of the mixing matrix $\mathbf{A}$. Corresponding to each $\mathbf{a}_j$ vector, it provides us the source signals $\mathbf{s}_i$, $i = 1 : N_s$, and each of them is a $1 \times N_t$ vector.

3. IMAGING BASED ON TIME REVERSAL-INDEPENDENT COMPONENT ANALYSIS (TR-ICA) METHOD

In a microwave imaging problem, one transmitting antenna propagates electromagnetic waves, and these waves after being scattered by the targets will be recollected by the receivers. Using the received signals we are able to construct a $N_r \times N_t$ observation matrix $\mathbf{K}$. Matrix $\mathbf{K}$ includes electromagnetic waves scattered by all of the scatterers. In performing the independent component analysis scatterers are considered as signal sources. Each of the receivers receives mixed signal from all the scatterers. Performing ICA we calculate $\mathbf{a}$ and $\mathbf{s}$ vectors corresponding to each scatterer. Then, $\mathbf{K}^{\text{target}}$ is defined separately for each scatterer as,

$$\mathbf{K}_j^{\text{target}} = \mathbf{a}_j \times \mathbf{s}_i \tag{11}$$

where each $\mathbf{K}_j^{\text{target}}$ is a $N_r \times N_t$ matrix ($j = 1, 2, \ldots, N_s$). After finding the appropriate matrix corresponding to each scatterer, $\mathbf{K}_j^{\text{target}}$ is applied to imaging the jth scatterer by back-propagation using Green's function. The Green's functions are in frequency domain, and $\mathbf{K}_{\text{target}}$ matrices are in time domain. Therefore, using the Fourier transform we map $\mathbf{K}_{\text{target}}$ matrices to frequency domain. Then using the mentioned matrix and vector Green's function, imaging can be done.

Vector Green's function connects an arbitrary point in the random medium to the receiving antenna and is defined as,

$$\mathbf{g}(\mathbf{x}_m, \omega) = [G(\mathbf{r}_1, \mathbf{x}, \omega) \ \ldots \ G(\mathbf{r}_{N_r}, \mathbf{x}, \omega)]^T \tag{12}$$

where the $\mathbf{r}_i$ is a space vector which shows the location of the ith receiving antenna, and $\mathbf{x}$ is a vector which shows the location of an arbitrary point in the random medium. Here, we have used the Green's function of random medium which is based on the Green's function of homogeneous medium and a mass operator (M) depending on the fluctuations of the random medium [19]. The fundamental equation for the Green's function of random medium is called the "Dyson Equation",

$$\left\langle G(\mathbf{r}, \mathbf{r}') \right\rangle = G_0(\mathbf{r}, \mathbf{r}') + \iint G_0(\mathbf{r}, \mathbf{r}_1) M(\mathbf{r}_1, \mathbf{r}_2) \left\langle G(\mathbf{r}_2, \mathbf{r}') \right\rangle d\mathbf{r}_1 d\mathbf{r}_2 \tag{13}$$

where $\mathbf{r}$ is position, $\langle\,\rangle$ the ensemble average, G_0 the free space Green's function and M the mass operator [19, 20]. The mass operator can be expressed by the following "Bourret" approximation,

$$M = \frac{k^4}{\epsilon_m^2} \left\langle G(\mathbf{r}_1, \mathbf{r}_2) \right\rangle \left\langle \epsilon_f(\mathbf{r}_1) \epsilon_f(\mathbf{r}_2) \right\rangle \tag{14}$$

The Dyson equation with (14) is called the first-order smoothing approximation.

By using the vector Green's function (12) and the signals in $\mathbf{K}^{\text{target}}$, we can scan the whole medium and do imaging as explained in the following. At any test point $\mathbf{x}_p$ in the medium, the function $P_p(\omega)$ can be calculated as,

$$P_p(\omega) = \mathbf{K}_{\text{target}}(\omega)^{-1} \mathbf{g}(\mathbf{x}_p, \omega) \tag{15}$$

Then, we again map $P_p(\omega)$ to time domain as,

$$P_p(t) = F^{-1}(P_p(\omega)) \tag{16}$$

where $F^{-1}(\cdot)$ is the inverse Fourier transform. In fact, we just back-propagated the signals using the Green's function of the medium. Now the final image can be calculated as,

$$I = \frac{P_p(t_f)}{|\max(P_p(t_f))|} \tag{17}$$

where t_f is the focusing time that the maximum of $P_p(t)$ at Equation (16) occurs in the medium. Plotting I for each $\mathbf{K}_j^{\text{target}}$ at all the points in the medium at time t_f provides us the image for the jth scatterer.

4. SIMULATION RESULTS

To do microwave imaging in a random medium based on TR-ICA, the first step is to simulate the electromagnetic waves propagating in the random medium. Then, by performing some processing and applying ICA algorithm, we are able to extract scatterers' information. In our simulations, we use a two-dimensional (2-D) FDTD code. The discretization grids are $\Delta x = \Delta y = 1\,\text{cm}$, and the total grid number is $N_x \times N_y = 124 \times 160$. The excitation signal is the first derivative of the wide-band *Blackman-Harris* (BH) [21] pulse that vanishes after a time period of $T = 1.55/f_c$ with $f_c = 400\,\text{MHz}$ as the central frequency. The medium in which the waves propagate is a random medium. In the model of the random medium which is based on [18], correlation lengths are on the order of a wavelength (resonant regime), so that the fluctuations are directly mapped into the FDTD domain.

We have used seven antennas as the receiving antennas which are shown by triangular markers and a transmitting antenna that is shown by a square marker. The conductivity and relative permeability of the medium is considered to be 0 and 1, respectively. Also there are two dielectric (or PEC) objects with a fixed $\epsilon_r = 15$ and radii of $r_1 = r_2 = 4\Delta x$ ($\approx 0.1\lambda$) centered at $(x_1, y_1) = (100, 70)\,\text{cm}$ and $(x_2, y_2) = (50, 140)\,\text{cm}$ (approximate distance of 2λ).

After recording the $\mathbf{K}$ matrix and applying ICA algorithm and post processing stages, the appropriate signal is propagated by the antennas which leads to focusing on the scatterers. In all of the figures in this section, the time reversed field back-propagated from the array is plotted. Also detecting the scatterers is done by finding the maximum value for the electric fields. To explore the effectiveness of the TR-ICA method, we have done several simulations in different imaging scenarios. We have also compared some of the TR-ICA results with the DORT method which is an established method in this domain. At the end, experimental results are also presented.

4.1. Selective Focusing on Extended Scatterers

In this example, focusing is done on electrically large scatterers (regarding to the wavelength). Figure 1 illustrates the detection of a target with diameter of 1λ. Compared to the results obtained by DORT method, TR-ICA shows more convincing result in detecting extended scatterers than DORT.

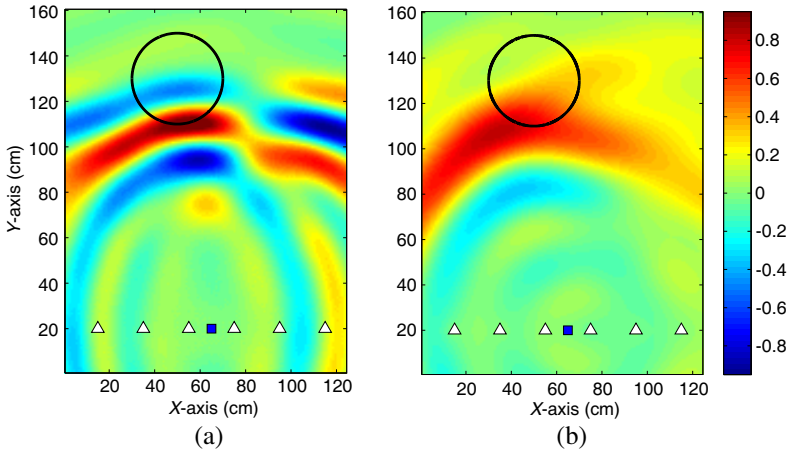

Figure 1. Focusing on an extended scatterer using (a) TR-ICA and (b) DORT method. The average permittivity (ϵ_m) of the random medium is 2.9 and variance (δ) is considered to be $0.0875\epsilon_m$. The target has circular cross section with diameter of 1λ. Receivers are located on a straight line at $y = 20\,\text{cm}$ separated 18 cm from each other. The only transmitter is at ($x = 65$, $y = 20$).

4.2. Selective Focusing on Close Scatterers

The main assumption for the TR-ICA method is the independence of the received scattered signals. In case the scatterers are close to each other, this assumption may not be valid anymore. We have done simulations focusing on dielectric scatterers with a short electrical distance between them. The size of

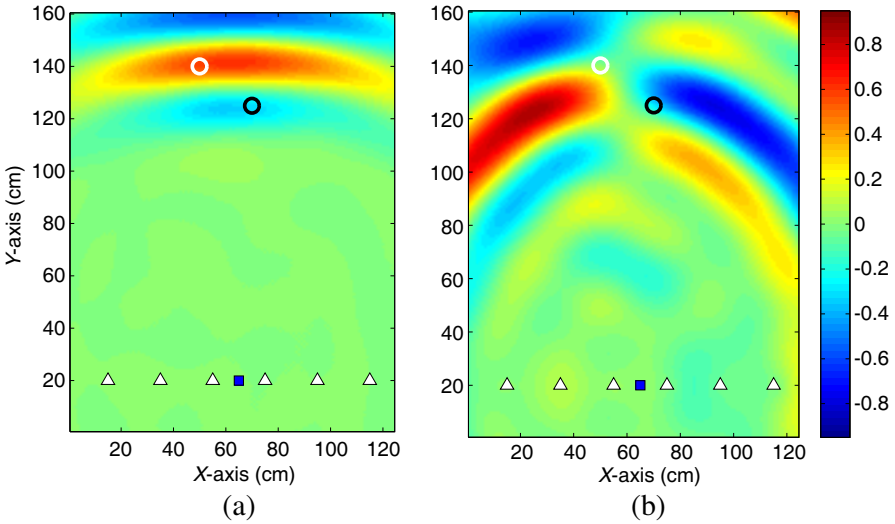

Figure 2. Focusing on the white scatterer using (a) TR-ICA and (b) DORT methods. The average permittivity (ϵ_m) of the random medium is 2.9 and variance (δ) is considered to be $0.0875\,\epsilon_m$. There are two dielectric scatterers in the medium with relative permittivity ($\epsilon_r = 15$).The size of scatterers is 0.1λ and the distance between the scatterers is $\approx 0.7\lambda$.

scatterers is 0.1λ which is considered to be electrically small. As can be seen in Figure 2, there is not a good focusing on the scatterers by DORT method while TR-ICA has a better functionality in detecting the objects. However, TR-ICA is not effective when the scatterers are closer than a distance of $\approx 0.7\lambda$. Figure 2 shows the performance of TR-ICA at this critical limit.

4.3. Selective Focusing in Multi-Scattering Medium

Multi-path propagation in a medium where several scatterers disturb the independency of the scattered signals from targets, which trouble the TR-ICA focusing. This is more crucial when the distance between the scatterers is electrically small. In the following figures (Figures 3, 4), the results of focusing

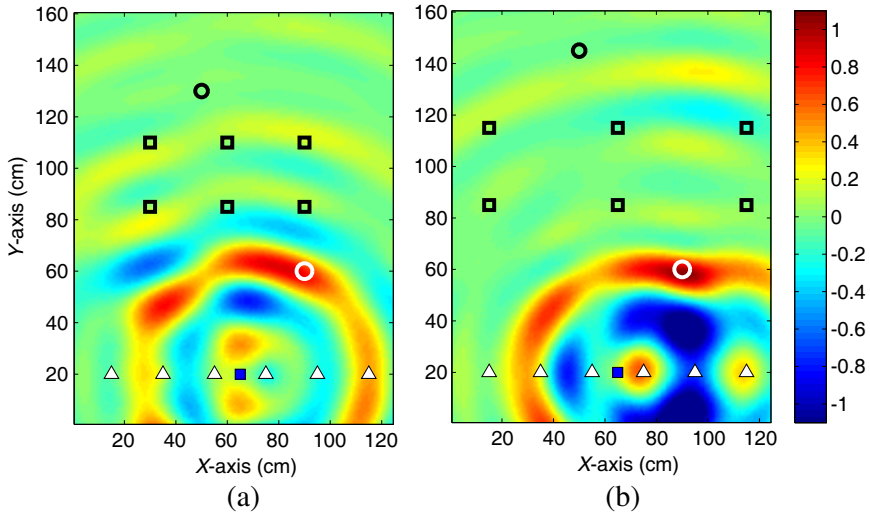

Figure 3. Focusing on the lower scatterer using TR-ICA method. The ϵ_m of the medium is 2.9 and variance (δ) is considered to be $0.0875\epsilon_m$. Here, there are two dielectric scatterers. Clutter objects are dielectric objects with a prescribed relative permittivity value of $\epsilon_r = 12$ and the main targets are specified by permittivity of $\epsilon_r = 20$. Focusing is done on the lower scatterer when there are (a) and (b) are two different configurations of the clutters.

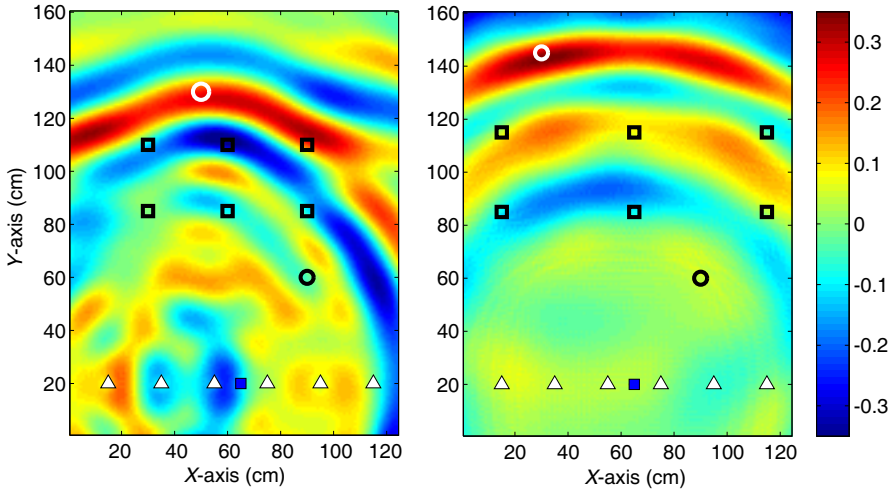

Figure 4. Focusing on the upper scatterer using TR-ICA method. The ϵ_m of the medium is 2.9 and variance (δ) is considered to be $0.0875\epsilon_m$. Here, there are two dielectric scatterers. Clutter objects are dielectric objects with a prescribed relative permittivity value of $\epsilon_r = 12$ and the main targets are specified by permittivity of $\epsilon_r = 20$. Focusing is done on the upper scatterer when there are (a) and (b) are two different configurations of the clutters.

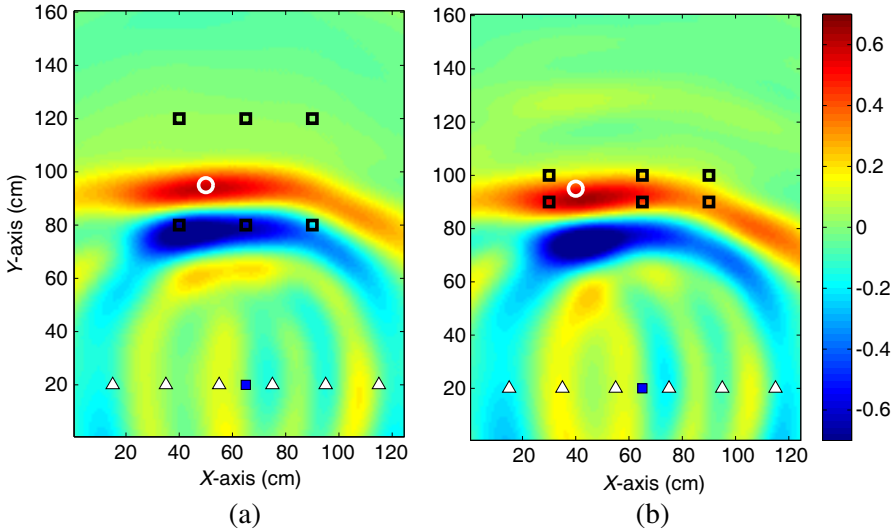

Figure 5. Focusing on the PEC scatterer using TR-ICA method. The ϵ_m of the medium is 2.9 and variance (δ) is considered to be $0.0875\epsilon_m$. Here, there is a PEC scatterer among dielectric clutters. Clutter objects are dielectric objects with a prescribed relative permittivity value of $\epsilon_r = 12$. (a) and (b) are two different configurations of the clutters.

on the dielectric scatterers in the presence of multi-scatterers (as clutter) are shown. Clutter objects are dielectric objects with a prescribed relative permittivity value of $\epsilon_r = 12$, and the main targets are specified by permittivity of $\epsilon_r = 20$.

In another scenario, we have considered a PEC scatterer among multiple clutters. Compared to the previous case, focusing is done more accurately on the PEC even in the case that the distances are short. Figure 5 shows the results.

In a more practical example, target and clutters are placed randomly in the medium. Figure 6 shows the result of the focusing on the target.

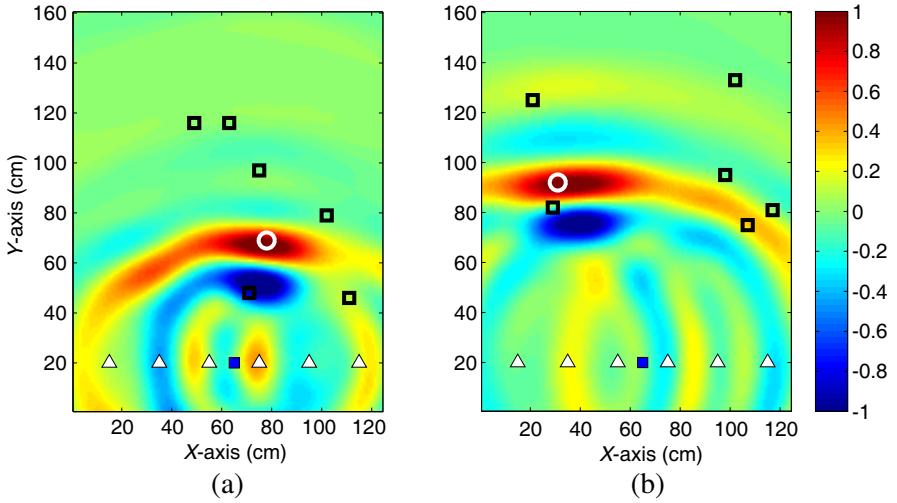

Figure 6. Focusing on the PEC scatterer using TR-ICA method. The ϵ_m of the medium is 2.9 and variance (δ) is considered to be $0.0875\epsilon_m$. Here, there is a PEC scatterer among random dielectric clutters. (a) and (b) are two different random clutter configurations.

4.4. Effect of Noise

In practical situations, different noise sources are present which contaminate the scattered signal. Based on our simulation results, adding noise to the medium (up to a limited value) does not disturb the results. In the coming Figures 7 and 8, a white Gaussian noise with a predefined power is added to the signals at the receivers, and the performance of the method is evaluated at different signal to noise ratios.

It is seen that when the noise source is located close to the scatterer (closer than $\approx 0.1\lambda$), it disturbs the performance much more than the case where the noise source is located far from the scatterer (a distance of $\approx 1\lambda$ or more). The crucial limit of the noise in our simulations is about -30 dBw when the noise source is located close to the scatterer and -15 dBw in the case the noise source is located far from the scatterers.

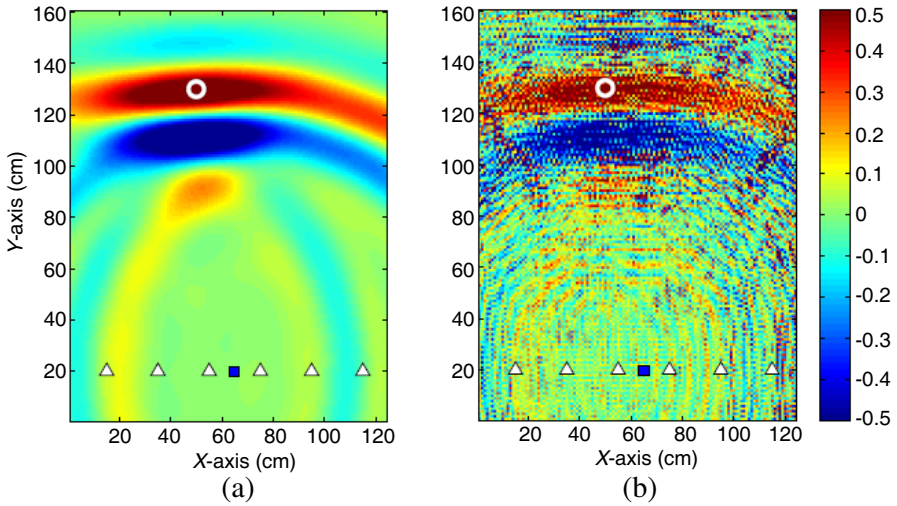

Figure 7. Focusing is done when (a) there is no noise (noiseless) and (b) the noise power level is -30 dBw. The noise source is close to the scatterer and far from antennas. The ϵ_m of the medium is 2.9 and variance (δ) is considered to be $0.0875\epsilon_m$. Here, there is a PEC scatterer.

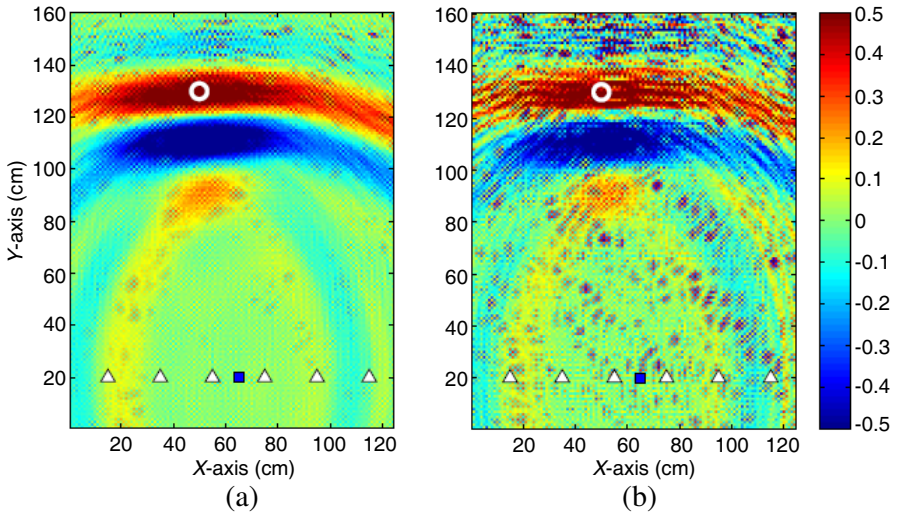

Figure 8. Focusing is done when the noise power level is (a) −30 dBw and (b) −15 dBw. The noise source is close to the antennas and far from the scatterer. The ϵ_m of the medium is 2.9 and variance (δ) is considered to be $0.0875\epsilon_m$. Here, there is a PEC scatterer.

4.5. Targets along Range Direction

Since we have only one transmitting antenna in case the targets are along the same direction perpendicular to the antenna array in front of the only transmitter antenna, the target closer to the transmitter overshadows the other one. Figure 9 shows the results focusing on PEC scatterers along the range direction.

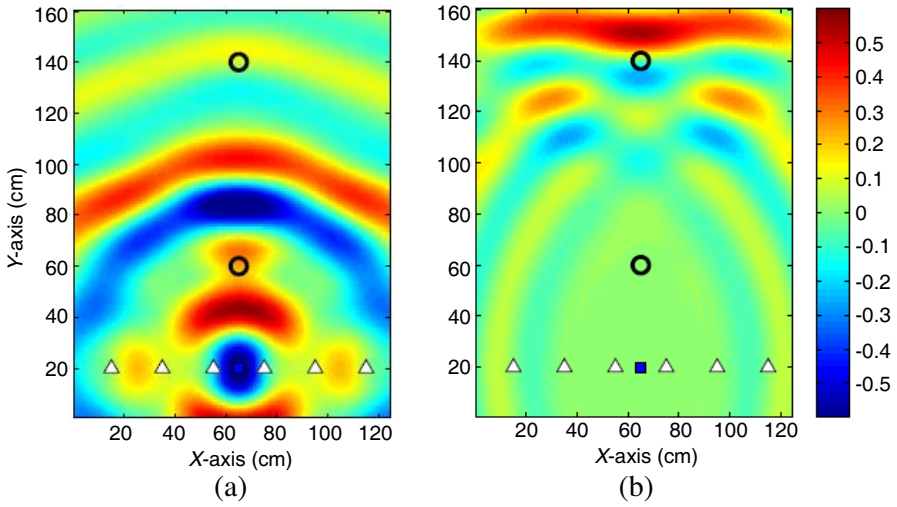

Figure 9. Focusing on the (a) lower scatterer and (b) upper scatterer in the case they are along the same direction perpendicular to the antenna array at the center antenna location.

4.6. Through the Wall Imaging

Through the wall imaging (TWI) determines the location of the target located on the opposite side of a wall with respect to the receiving and transmitting antennas. Several effective TWI algorithms have addressed this problem [22, 23]. In this section, we focus on TWI within the framework of time reversal applying ICA technique for the decomposition of the received scattered signals.

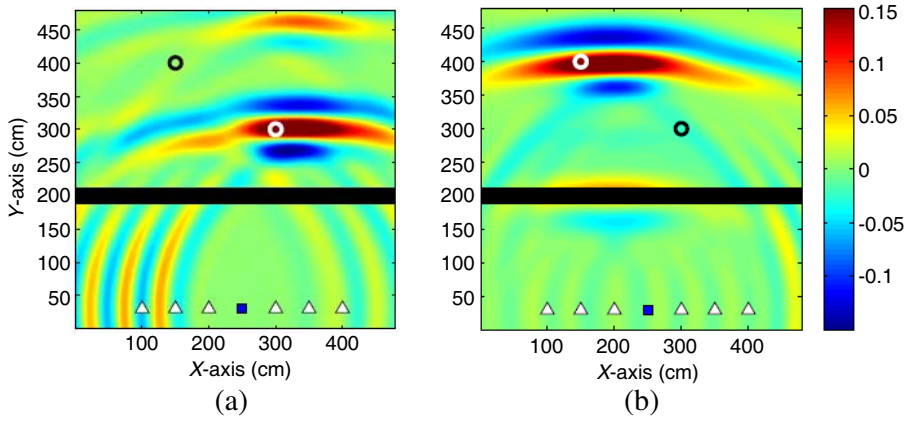

Figure 10. Focusing on the (a) first scatterer and (b) second scatterer. The ϵ_m of the medium is 2.9 and variance (δ) is considered to be $0.0875\epsilon_m$. There are two PEC scatterers behind the wall.

Here, the total grid number is $N_x \times N_y = 500 \times 500$. There are two point-like static cylindrical conductor objects behind the wall at locations $x_{m1} = (150, 400)\,\text{cm}$ and $x_{m2} = (300, 300)\,\text{cm}$ (the distance of 4λ) with radii $R1 = 15\Delta x (\approx 0.35\lambda)$ and $R2 = 22\Delta x (\approx 0.5\lambda)$. We consider a uniform linear array of 7 elements centered at the position r_j at a distance of $\approx 150\,\text{cm}$ in front of the wall, where, $j = 1, 2, \ldots, 7$, $r_j = (x_j, y_j)$. The receiver antenna elements are placed with an inter-element spacing of $\Delta x = 50\,\text{cm} \approx 1\lambda$ and $r_1 = (x_1, y_1) = (100, 30)\,\text{cm}$. The only transmitting antenna is placed at the center of the array. Also the wall is homogeneous with parameters, $\epsilon_r = 8$ and $\sigma = 0.01\,\text{S/m}$, and thickness, $d = 20\,\text{cm}$. Triangles show the locations of receivers, and circles show the locations of scatterers. The only transceiver antenna is shown by a blue square marker. As can be seen in Figure 10, selective focusing is done properly on each scatterer.

5. EXPERIMENTAL TIME REVERSAL INDEPENDENT COMPONENT ANALYSIS (TR-ICA) MICROWAVE IMAGING

We have prepared an experimental setup to test the TR-ICA method. Two similar antennas are used for measurements. One of them is transmitter and receiver, and the other is only receiver. The transmitter/receiver antenna is placed at a fixed location, and the receiving antenna is placed at six different locations during a measurement set. There are 5 scatterers which are 50 cm long dielectric rods made of teflon ($\epsilon_r \approx 2.1$) and two similar PEC targets located on a board. Horn antennas are used as transmitting and receiving antennas. The antennas are plugged into an Agilent L5222A PNA network analyzer. A picture of the experiment setup is shown in Figure 11. We have measured the scattered

Figure 11. View of the experiment setup with antennas and targets.

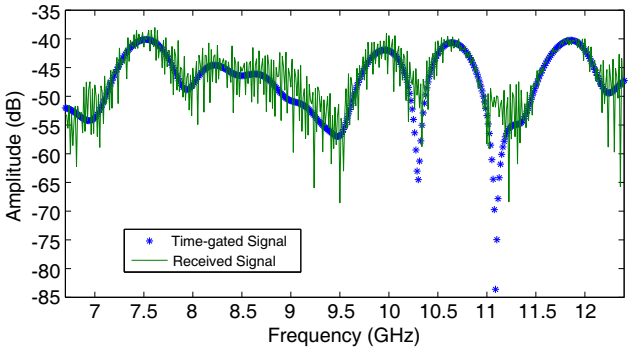

Figure 12. The received signal from the first antenna in the cases of gated and not gated.

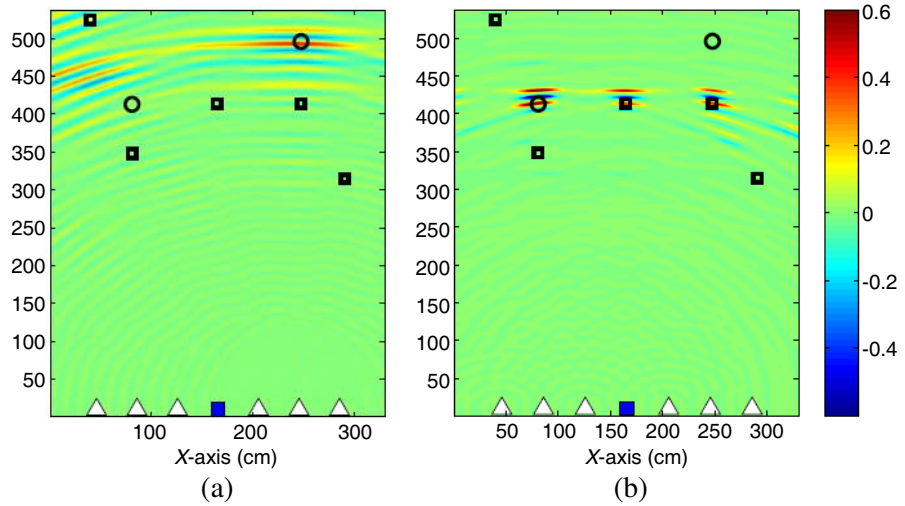

Figure 13. Focusing on the (a) first scatterer and (b) second scatterer. There are two PEC targets in a random medium among multi dielectric scatterers. PEC targets are shown by circular marks and dielectric scatterers are shown by rectangular marks.

signals at six different locations of the receiver antenna and one measurement with both transmitter and receiver at one location. The measurements are done in the frequency range between 6.7 to 12.4 GHz containing 457 equi-spaced frequency samples. The spacing between the antenna locations is 15 cm which is equal to 3.3λ at a frequency of 6.7 GHz. Also the distance between the targets and the transmitter antenna is 90 cm while the average spacing between the scatterers on the board is 12 cm or $\approx 3\lambda$ (refer to Figure 11). After recording the K matrix using the time-gated signals we applied ICA algorithm and post processing steps. As shown in Figure 12, the time gating is done on the signals in order to compensate for the multi-scattering by room walls and setup structure. Finally, the appropriate signal is synthetically propagated through the medium using a FDTD simulation. The selective focusing on the targets is done successfully and depicted in Figure 13.

The experimental results in Figure 13 show that TR-ICA has effectively identified the targets.

6. CONCLUSION

In this paper, we have introduced a new time reversal imaging method which is based on the independent component analysis (ICA) for decomposing mixed signals back scattered from targets. We have done several simulations to investigate the effectiveness of the TR-ICA method for imaging. Imaging scenarios, such as small dielectric scatterers, extended scatterers, multi-scattering environment, noisy medium and TWI, are investigated. Also the simulation results are verified by some experiments. Based on the simulation results and experiments, the introduced method is effective in all the simulated situations. Some of the results are also compared to the DORT method. Only one transmitting antenna is used in TR-ICA method. The main advantage of the TR-ICA method over other techniques is that we are able to achieve better or comparable results with less hardware and computational load.

REFERENCES

1. Prada, C. and M. Fink, "Eigenmodes of the time reversal operator: A solution to selective focusing in multipletarget media," *Wave Motion*, Vol. 20, 151–163, September 1994.
2. Fink, M., D. Cassereau, A. Derode, C. Prada, P. Roux, M. Tanter, J. L. Thomas, and F. Wu, "Time-reversed acoustics," *Reports on Progress in Physics*, Vol. 63, No. 12, 1933–1995, 2000.
3. Fouda, A. E. and F. L. Teixeira, "Imaging and tracking of targets in clutter using differential time-reversal techniques," *Waves in Random and Complex Media*, Vol. 22, No. 1, 2012.

4. Kosmas, P. and C. Rappaport, "Time reversal with the fdtd method for microwave breast cancer detection," *IEEE Transactions on Microwave Theory and Techniques*, Vol. 53, 2317–2323, July 2005.
5. Kosmas, P. and C. Rappaport, "FDTD-based time reversal for microwave breast cancer detection-localization in three dimensions," *IEEE Transactions on Microwave Theory and Techniques*, Vol. 54, 1921–1927, June 2006.
6. Yavuz, M. and F. Teixeira, "Full time-domain dort for ultrawideband electromagnetic fields in dispersive, random inhomogeneous media," *IEEE Transactions on Antennas and Propagation*, Vol. 54, No. 8, 2305–2315, 2006.
7. Lehman, S. K. and A. J. Devaney, "Transmission mode time-reversal super-resolution imaging," *The Journal of the Acoustical Society of America*, May 2003.
8. Yavuz, M. and F. Teixeira, "Space frequency ultrawideband time-reversal imaging," *IEEE Transactions on Geoscience and Remote Sensing*, Vol. 46, No. 4, 1115–1124, 2008.
9. Scholz, B., "Towards virtual electrical breast biopsy: Space-frequency music for trans-admittance data," *IEEE Transactions on Medical Imaging*, Vol. 21, No. 6, 588–595, 2002.
10. Razavian, M., M. Hosseini, and R. Safian, "Time-reversal imaging using one transmitting antenna based on independent component analysis," *IEEE Geoscience and Remote Sensing Letters*, Vol. 11, No. 9, 1574–1578, 2014.
11. Comon, P., "Independent component analysis, a new concept?," *Signal Processing*, Vol. 36, No. 3, 287–314, Higher Order Statistics, 1994.
12. Jutten, C., "Source separation: From dusk till dawn," *2nd Int. Workshop on Independent Component Analysis and Blind Source Separation*, 15–26, 2000.
13. Jutten, C. and J. Herault, "Blind separation of sources, Part I: An adaptive algorithm based on neuromimetic architecture," *Signal Processing*, Vol. 24, No. 1, 1–10, 1991.
14. Hyvrinen, A., J. Karhunen, and E. Oja, *Independent Component Analysis*, John Wiley & Sons, Inc., May 2001.
15. Bell, A. J. and T. J. Sejnowski, "An information-maximization approach to blind separation and blind deconvolution," *Neural Computation*, Vol. 7, 1129–1159, April 2008.
16. Cardoso, J.-F. and A. Souloumiac, "Blind beamforming for non-Gaussian signals," *IEE Proceedings F (Radar and Signal Processing)*, Vol. 140, 362370, December 1993.
17. Hyvarinen, A., "Fast and robust fixed-point algorithms for independent component analysis," *IEEE Transactions on Neural Networks*, Vol. 10, No. 3, 626–634, 1999.
18. Moss, C., F. Teixeira, Y. Yang, and J.-A. Kong, "Finite-difference time-domain simulation of scattering from objects in continuous random media," *IEEE Transactions on Geoscience and Remote Sensing*, Vol. 40, No. 1, 178–186, 2002.
19. Ishimaru, A., "Wave propagation and scattering in random media and rough surfaces," *Proceedings of the IEEE*, Vol. 79, No. 10, 1359–1366, 1991.
20. Frisch, U., "Wave propagation in random media," *Probabilitistic Methods in Applied Mathematics*, 1968.
21. Harris, F., "On the use of windows for harmonic analysis with the discrete fourier transform," *Proceedings of the IEEE*, Vol. 66, No. 1, 51–83, 1978.
22. Zhang, W., A. Hoorfar, and L. Li, "Through-the-wall target localization with time reversal MUSIC method," *Progress In Electromagnetics Research*, Vol. 106, 75–89, 2010.
23. Bardak, C. and M. Saed, "Through the wall microwave imaging using fdtd time reversal algorithm," *2013 IEEE Antennas and Propagation Society International Symposium (APSURSI)*, 528–529, July 2013.